

A Dual-Armed Robotic System for Intraoperative Ultrasound Guided Hepatic Ablative Therapy: A Prospective Study

Emad M. Boctor¹, Gregory Fischer¹, Michael A. Choti², Gabor Fichtinger¹, Russell H. Taylor¹

¹Engineering Research Center ERC-CISST, The Johns Hopkins University, Baltimore MD, USA;

²Department of Surgery, The Johns Hopkins University, Baltimore MD, USA

E-mail: {eboctor, gfisch}@ieee.org, mchoti@jhmi.edu, {GaborF, rht}@jhu.edu

Abstract— There has been increased interest in minimally invasive ablative treatments that typically require precise placement of the ablator tool to meet the predefined planning and lead to efficient tumor destruction. Standard ablative procedures involve free hand transcutaneous ultrasonography (TCUS) in conjunction with manual tool positioning. Unfortunately, existing TCUS systems suffer from many limitations and result in failure to identify nearly half of all treatable liver lesions. Freehand manipulation of the ultrasound (US) probe and ablator tool lacks the critical level of control, accuracy, stability, and guaranteed performance required for these procedures. Freehand US results in undefined gap distribution, anatomic deformation due to variable pressure from the sonographer's hand, and severe difficulty in maintaining optimal scanning position. In response to these limitations, we propose the use of a dual robotic arm system that manages both ultrasound manipulation and needle guidance. We report a prototype of the dual arm system and a comparative performance analysis between robotic vs. freehand systems, for both US scanning and needle placement in mechanical and animal tissue phantoms.

Keywords—Image Guided Surgery; Robotic Needle Placement; Robotic Ultrasound; 3D Ultrasound; Thermal Ablation; Tracking; Image Guided Therapy

I. BACKGROUND AND SIGNIFICANCE

Hepatocellular carcinoma presents over 1 million cases per year worldwide [1]. Liver is the most frequent location of metastasis from colorectal cancer, representing 130,000 new cases and 60,000 deaths in the US alone. Current treatment for liver cancer includes resection of part of the liver and ablative treatment. Unfortunately, most patients with primary and secondary liver cancer are not candidates for resection, primarily due to tumor location or underlying liver disease.

For these reasons, an increasing interest has been focused on interstitial ablative approaches for the treatment of unresectable liver tumors. In addition to increasing the number of patients eligible for curative therapy of liver cancer, local tissue ablation is performed with lower

morbidity than resection. It is very suitable for percutaneous and other minimally invasive approaches. Because many tumors cannot be seen with TCUS, minimally invasive percutaneous therapy may be ineffective at removing all malignant growths. One research approach to compensate for poor visibility in TCUS is registration of preoperative MRI/CT to TCUS [2]. However, as Russo *et al.* note, "the diagnostic accuracy of alternative techniques, i.e. preoperative imaging (angiography, Scintigraphy, CT, ultrasonography), and surgical exploration, doesn't exceed 60-80%. Intraoperative ultrasonography (IOUS), however, allows for early diagnosis and precise localization of many diseases, and it is an excellent guidance tool for accurate and radical surgical treatment." Intraoperative and laparoscopic ultrasonography both can provide both excellent real-time anatomical imaging and have been found most beneficial in a multitude of interventions.

In current clinical practice, IOUS guided liver ablation is typically performed in two steps. First, the target tumors are identified in preoperative imaging, typically in CT or MRI. Second, these tumors are intra-operatively localized by means of IOUS. However, the two-dimensional nature of IOUS imaging leads to significant variations in results among users. Simultaneous manual handling of the IOUS probe and the ablator device is a challenging task that is prone to significant errors in the hands of even the most experienced physicians. Respiratory motion and liver surface deformation are two of the most significant sources of error. Galloway *et al.* used IOUS and a laser ranger for better registration and assessment of liver motion and deformation [16]. Jane Mary *et al.* built respiratory motion models that help in registering preoperative MRI/CT to IOUS [6]. Other solutions include real-time deformation modeling coupled with conventional tracker-based surgical navigation [15].

Compounding the collected 2D images into a 3D volume provides an excellent tool for intra-operative planning, but it is extremely difficult to achieve by freehand scanning. A robot-assisted ultrasound system would provide significant benefit by enabling more structured and optimized 3D

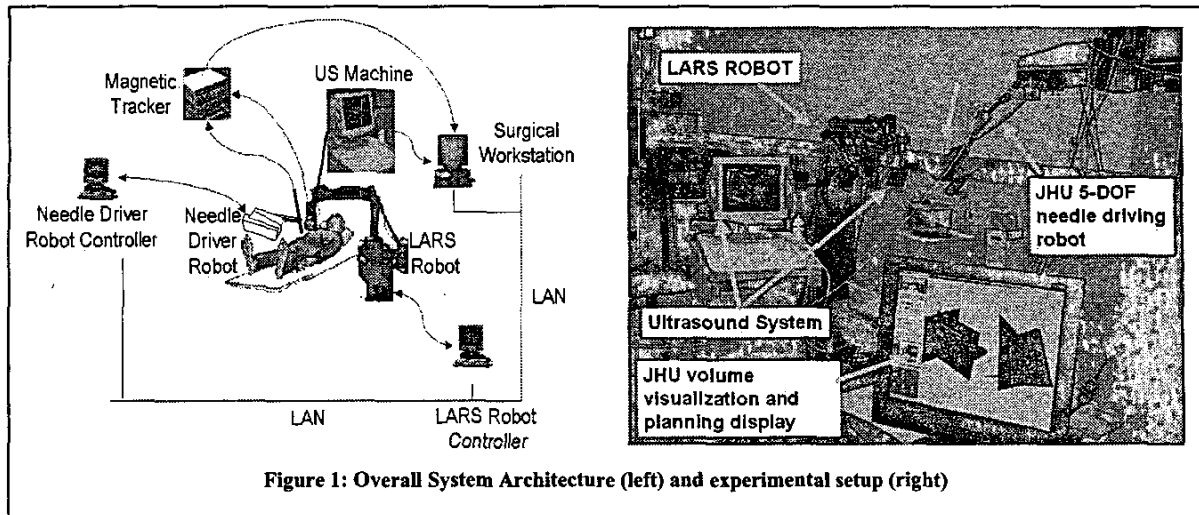


Figure 1: Overall System Architecture (left) and experimental setup (right)

ultrasound datasets, providing consistent reliable guidance to interventions, and avoiding fatigue and occasional musculo-skeletal injury of the sonographer [4]. In liver ablation surgery, robot-assisted ultrasound can also maintain the pressure profile induced by the US probe, thus minimizing tissue deformation and motion artifacts. Several groups have been exploring robotic assistance for ultrasonography (e.g., [5], [7]).

Freehand handling and aligning of the surgical tool to follow a planned trajectory is also a challenging task. This task requires manipulation of the tool, while at the same time observing the motion on a monitor. Even for the experienced surgeon, performance and reliability is not guaranteed. Therefore, there has been a recent interest in US-guided, robotically assisted, needle placement by several groups (e.g., [8]), including our team [9].

In this paper, we are reporting on a “two handed” system in which robot arms manipulate both the ultrasound and needle placement devices, in the surgical context of liver cancer biopsy and ablation. This system may allow for superior US imaging and placement of the tool tip, compared to that of freehand ultrasonography and needle placement. The dual-arm configuration assists the surgeon in device manipulation and hand-eye coordination, so that more effort can be concentrated on planning and monitoring the procedure. By promoting more accurate imaging and targeting of the lesions, we potentially improve the therapeutic coverage of those cancerous regions and reduce the number of needle insertions required, thus reducing the likelihood of spreading cancer along a needle path.

II. EXPERIMENTAL SYSTEM

A. System Overview

Figure 1 shows the overall architecture of our experimental system, and Figure 2 shows the experimental setup in our laboratory. Major system components include:

- A PC-based surgical workstation providing overall application control, 2D and 3D ultrasound processing and surgeon interfaces.
- A conventional 2D ultrasound system (SSD-1400 ultrasound machine, Aloka Inc.) interfaced to the surgical workstation.
- A robot (the IBM/JHU LARS) holding the ultrasound probe.
- A second robot for positioning a needle guide.
- An electromagnetic (EM) tracking system (Flock of Birds, model 6D FOB, Ascension Technology, Inc.) interfaces to the surgical workstation.

In providing positional reference and co-registration between the ultrasound and ablator needle, we rely on an electro-magnetic tracking system rather than the robot encoders. The tracker base unit is fixed to the operating table, and individual sensors are attached to the ultrasound probe and needle guide. The main advantages of this approach are: (1) it permits quick reconfiguration of the experimental setup to use 0, 1, or 2 robots, and (2) it simplifies modular replacement of end effectors. With this

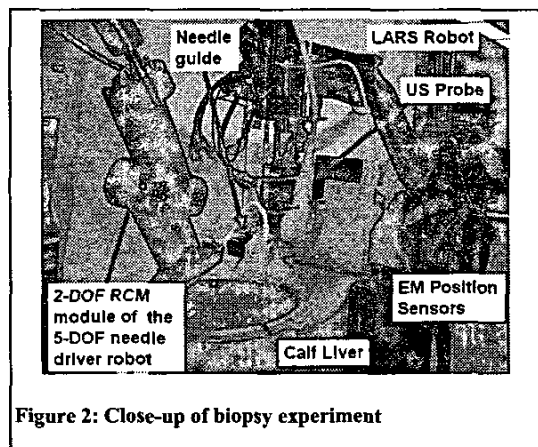


Figure 2: Close-up of biopsy experiment

approach, we must calibrate only the tool tips (US and needle) to the tracker, and the motion of both robots is based entirely on sensed tool location [10]. As neither robot accomplishes motion through inverse kinematics, the robots do not need to be pre-calibrated to tracker space.

B. Ultrasound robot

In the current prototype, we use an IBM/JHU LARS robot [11] for US guidance, as shown in Figure 2. This system was originally designed for precise, minimally invasive surgery. It has a three axis Cartesian base, a two axis "remote center-of-motion" (RCM) linkage, and a two axis instrument carrier providing a third axis of rotation about an instrument shaft and a translational motion toward or away from the RCM point. The reasons for this choice are availability, ability to control from within our robot control software (<http://www.cisst.org/resources/software/mrc>), and its RCM design that facilitates reorientation motions of the ultrasound probe. The RCM design is also attractive considering our long-term plan of using laparoscopic ultrasound. The ultrasound probe is mounted on the instrument carrier of the robot, as shown in Figure 2. The LARS instrument carrier is equipped with a six degree-of-freedom (DOF) force/torque sensor, which is useful in controlling probe-tissue interaction forces and moving the robot under cooperative control. This takes the form of compliance guiding in a manner similar to our "Steady Hand" guidance system for microsurgical robotic assistance [12]. The LARS uses a custom PC-based controller running our MRC robot control software.

C. Needle driver robot

The needle driver robot, shown in Figure 1 and partially in Figure 2, consists of a 3 axis Cartesian stage, an adjustable clamping device (passive arm), and a JHU chain drive RCM module [13]. The needle insertion module is not powered and it serves as a passive needle guide. Like the LARS, this robot too has its custom PC-based controller running our MRC robot control library.

D. Surgical Workstation

The surgical workstation is a 700 MHz Pentium-3 computer with 512 MB of main memory, running the Windows NT operating system. This workstation is the central hub of our experimental setup, and is interfaced to the ultrasound system, the EM tracking system, and both robot controllers. It runs custom software implemented on top of the 3D Slicer medical data visualization package. 3D Slicer is a public domain, open source system primarily developed by the Surgical Planning Laboratory at the Brigham and Women Hospital (<http://www.slicer.org>), with sustained contribution from our group at JHU. This software environment is used to:

- Acquire 2D ultrasound (2DUS) ultrasound images and combine them into a 3D ultrasound (3DUS)

volume [3] based on 6 DOF pose data from the EM sensor attached to the ultrasound probe. Calibration of the 2DUS images to the EM sensor was performed using our method [14].

- Tracking the needle position and orientation with respect to the 3DUS volume in real-time.
- Plan the needle entry points and target points. For ablation applications, this software also includes facilities for planning overlapped ablation volumes.
- Visualize the needle position and plan parameters with respect to the 3DUS volume.

Figure 3 shows a typical planning screen in 3D Slicer showing the chosen entry and target points (the red and green spheres respectively) with the surgical tool superimposed over them. Individual slices along each axis may also be viewed for precise planning, as shown in Figure 4. These two figures represent 3DUS of a calf liver with olives implanted and used as targets.

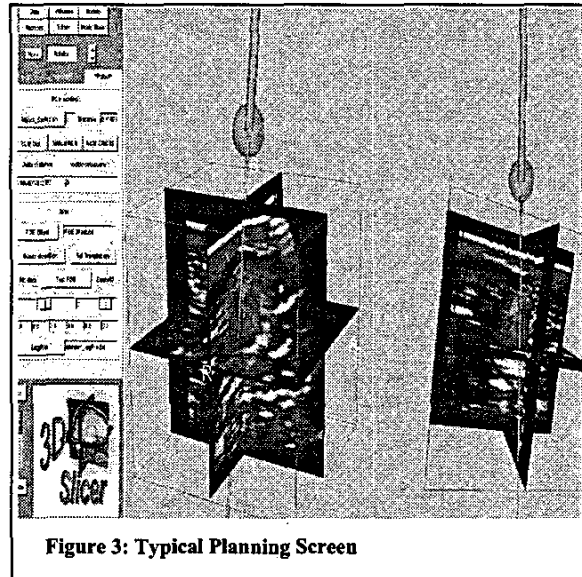


Figure 3: Typical Planning Screen

III. EXPERIMENTAL PROCEDURE

We conducted needle placement experiments using three different phantoms. The first phantom was a slightly overripe plum immersed in a water tank and the plum's pit served as the target. The second phantom was a calf liver with pitted olives embedded in the liver at depths ranging from 5 mm to 40 mm, to simulate cancerous lesions. Figure 2 and 5 show close-ups of the apparatus with the liver phantom.

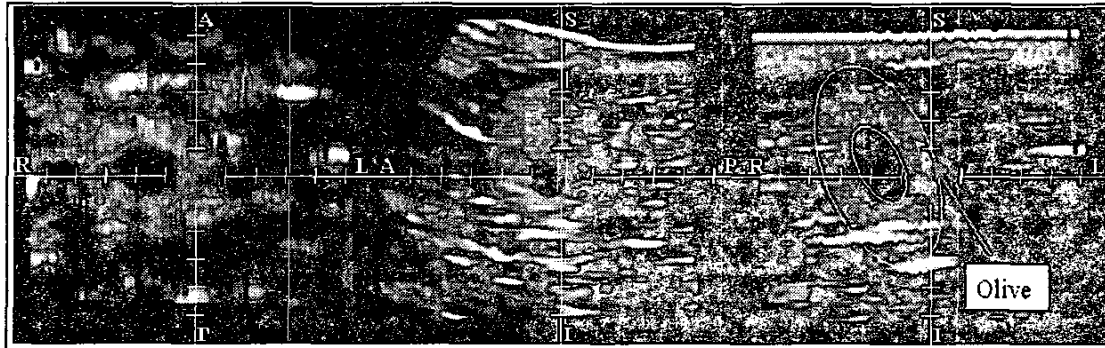


Figure 4: Orthogonal slices of 3DUS reconstruction of an olive in calf liver phantom

In order to assess the geometric accuracy of the system a third, mechanical phantom was introduced. This phantom, shown in Figure 6, consists of several plastic pins (8 mm OD) immersed in a water tank. We also used this phantom to compare the performance of our dual-arm system to single-arm scenario performing either US scanning or needle insertion. Next we will describe the workflow for the liver phantom, noting that the procedure was almost identical for the other two phantoms.

Step 1: Exploration. We use the LARS robot in either force compliant or teleoperation mode to move the US probe over the liver. Concurrently, we observe the live 2DUS images to approximate target volume of interest (VOI) containing target lesions. Then we command the LARS to move the US probe between the start and end points of the VOI. In essence, we “teach” the LARS controller the scanning protocol for the given VOI.

Step 2: Volume Scanning. The LARS autonomously moves the US probe from the start to the end points in a step-and-repeat fashion, with 20 ms pauses at each step. (In this experiment, we applied one-dimensional translational scanning motion.) At each position, a 2DUS image is acquired along with the EM pose information. Our system is also capable of acquiring images with a continuous motion scan, but we preferred step-and-repeat mode to make the synchronization between the EM tracker and the US unit more accurate. The 2DUS images are then compounded into a 3DUS volume. Figure 4 depicts three orthogonal slices passing through the center of an olive target.

Step 3: Planning. The interactive 3D Slicer interface is used to identify the target and entry points. The display shows the trajectory of the needle and the predicted region of ablation. The computer also determines the insertion depth for the needle.

Step 4: Needle robot motion. A depth marker is placed on the needle at the appropriate distance from the tip, and then the needle is placed into the guide. The 5 DOF needle placement robot moves the needle tip over the entry point and aligns the needle in the desired path in three steps: (1) orient the needle approximately while the robot is still in some safe distance from the subject; (2) move the needle tip to the entry point; and (3) align the needle precisely using the RCM stage.

Step 5: Insertion. The needle is driven manually to the predetermined depth, monitored by the depth marker and in the real-time computer display. During both insertion and assessment, either the US probe on the LARS or a stand-alone probe (Figure 5) is used to monitor and confirm placement of the needle.

Step 6: Assessment. We record (1) whether we hit the target and (2) the insertion depth at which the needle actually hits the target. We also use a second ultrasound probe to observe the needle tip, and to target and measure the distance between them with the standard operator’s interface on the ultrasound console. Figure 5 shows the procedure and a typical US image.

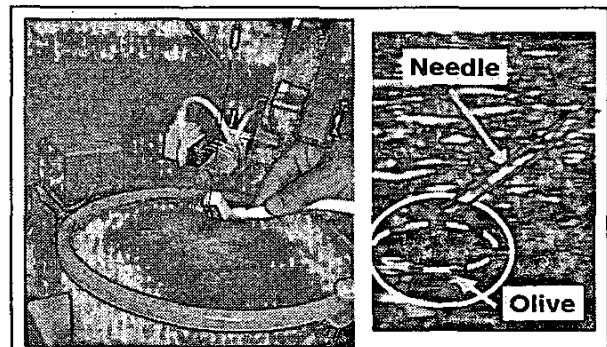


Figure 5: Ultrasound is used to assess needle placement with respect to the olive target embedded in calf liver

IV. RESULTS AND DISCUSSION

We have conducted three successful experiments for the liver/olive phantom procedure described before. Verification has been done in two of them by feeling the resistance of the olive and in the last one by observing the US image, Figure 5. Based on three measurements, the average mismatch between real and planned insertion depths was of 1.2 mm.

We collected three robotic scans and three freehand scans for the mechanical phantom shown in Figure 6, to compare the performance of robot-assisted needle insertion with and without robotic US scan. First, we selected a VOI containing the targets and reconstructed the VOI into a 3DUS volume for needle insertion planning. The ratio of the number of raw 2DUS pixels within the VOI to the number of voxels in the VOI was compared. For reconstructions from a single robotic sweep, this ratio was consistently about 1.5-1.6, while the ratio for a single freehand sweep was between 0.3-0.8, an inconsistent value, fluctuating in a wide range. Increasing the number of freehand sweeps to three, the ratio still remains approximately only 0.9, still with considerable variability. A ratio greater than 1.0 may imply that we either have relatively little gap between the slices, or we try to place multiple pixels in the same voxel, either case leading to better 3D image quality. In our experiments for freehand scanning, this ratio was found to be less than 1.0 and rather inconsistent, implying that we had many empty voxels in the volume, either because of scanning gaps or because of the orientation of scan plane within the reconstructed volume. In either case, a lower image quality can be observed, compared to robot-assisted scans, and there is also a strong indication that repeated scans cannot be consistently acquired freehand.

To determine the systemic error of the dual-arm system on the mechanical phantom, we placed the tracked needle at the artificial target (plastic pin) and recorded the distance between the needle tip and the target in the Slicer screen. From 10 trials, the average measure was ~3.0 mm. This measurement of error comprised the all the elements of the system error (except the error of the robot control algorithm and needle deflection in real tissue): US calibration (0.8 mm), calibration error of needle tip to tracker, sensor uncertainty (2.54 mm), floating point truncation (1-2 pixels), and US image resolution. For termination criterion, the robot control algorithm (which is described in detail in a companion paper [10]) used the system error we found above. Using robotic needle insertion with robotic US data, the success rate in hitting the head of the pin was 7 out of 7 trials. Using robotic insertion with freehand US data, the success rate was only 3 out of 4 trials. This could be explained because of: 1) the presence of gaps that degrade the planning accuracy, and/or 2) the synchronization inaccuracy due to dynamic tracking of freehand system.

In future work, more phantom studies, followed by in vivo animal trials need to be conducted before clinical trials can be considered. We will also conduct a comparative study of system embodiments with two robots, one robot, and no robot. For those experiments, we will upgrade the EM tracker to a more accurate device such as an Optotrak (NDI,

Inc.) and also utilize more sophisticated motion planning methods, such as including virtual fixtures in the vicinity of critical anatomical structures.

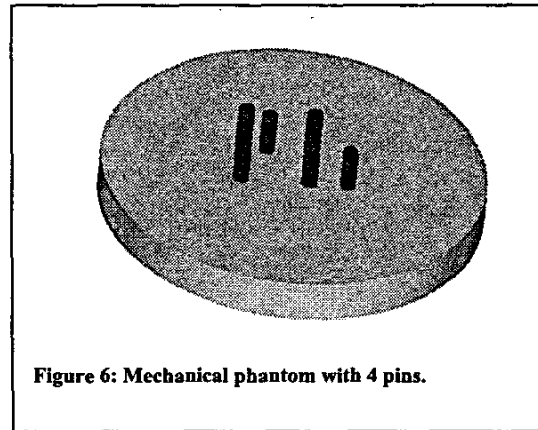


Figure 6: Mechanical phantom with 4 pins.

ACKNOWLEDGMENT

The authors acknowledge the support of the National Science Foundation under the Engineering Research Center grant #EEC-9731478. We would also like to thank Aloka for their support and Dr. Dan Stoianovici for maintenance of the RCM mechanism.

REFERENCES

- [1] Nakakura, E. and M. Choti, *Hepatocellular Carcinoma: Current Management Recommendations*. *Advances on Onc*, 2000. 16(2): p. 12-18.
- [2] Penney, G.P., et al. *Overview of an Ultrasound to CT or MR Registration System for use in Thermal Ablation of Liver Metastases*. in *Medical Image Understanding and Analysis*. 2001. Birmingham, England
- [3] Boctor, E., et al. "Tracked 3D ultrasound in radio-frequency liver ablation." *Proc. SPIE Vol. 5035*, p. 174-182, *Medical Imaging 2003: Ultrasonic Imaging and Signal Processing*; William F. Walker, Michael F. Insana; Eds.
- [4] Vanderpool, H.E., et al., *Prevalence of carpal tunnel syndrome and other work-related musculoskeletal problems in cardiac sonographers*. *Journal of Occupational Medicine*, 1993. 35: p. 604-610.
- [5] Abolmaesumi, P., et al., *Image-Guided Control of a Robot for Medical Ultrasound*. *IEEE Transactions on Robotics and Automation*, 2002.
- [6] Jane Mary Blackall, "Respiratory Motion in Image Guided Intervention of Liver," Ph.D. Thesis Sep2002, King's College London.
- [7] Adriana Vilchis, Jocelyne Troccaz, Philippe Cinquin, Agnes Guerraz, Franck Pellissier, Pierre Thorel, Bertrand Tondou, Fabien Courrèges, Gérard Poisson, Marc Althuser, and Jean-Marc Ayoubi, "Experiments with the TER tele-echography robot," *MICCAI 2002, LNCS 2488*, pp. 138-146, 2002.
- [8] Hong, J.S., et al. *A Motion Adaptable Needle Placement Instrument Based on Tumor Specific Ultrasonic Image Segmentation*. in *Medical Image Computing and Computer-Assisted Intervention - MICCAI 2002. LNCS 2488*, p.9-16.

- [9] Fichtinger, G., et al., *Robotically-assisted prostate brachytherapy with transrectal ultrasound guidance – preliminary experiments*. Journal of Medical Physics. (in review).
- [10] Bector, E.M., et al. "Virtual Remote Center of Motion Control for Needle Placement." in Medical Image Computing and Computer-Assisted Intervention - MICCAI 2003(accepted).
- [11] Taylor, R.H., et al., *A Telerobotic Assistant for Laparoscopic Surgery*. IEEE Engineering in Medicine and Biology Magazine, 1995. 14: p. 279-287.
- [12] Taylor, R., et al., *A Steady-Hand Robotic System for Microsurgical Augmentation*. International Journal of Robotics Research, 1999. 18(12).
- [13] Stoianovici, D., et al. *A Modular Surgical Robotic System for Image-Guided Percutaneous Procedures*. in Medical Image Computing and Computer-Assisted Interventions (MICCAI-98).11-13 p.404-410.
- [14] Bector, E., et al. "Rapid calibration method for registration and 3D tracking of ultrasound images using spatial localizer." Proc. SPIE Vol. 5035, p. 521-532, Medical Imaging 2003: Ultrasonic Imaging and Signal Processing; William F. Walker, Michael F. Insana; Eds.
- [15] M. Vetter, P. Hassenpflug, M. Hastenteufel, I. Wolf, M. Thorn, L. Grenacher, G. M. Richter, W. Lamade, W. Uhl, M. W. Buechler, and H. Meinzer, "Real-time deformation modeling and navigation aids for open liver surgery," Proc. SPIE Vol. 5029, p. 58-68, Medical Imaging 2003: Visualization, Image-Guided Procedures, and Display; Robert L. Galloway, Jr.; Eds.
- [16] David M. Casha, Tuhin K. Sinha, William C. Chapman, Hiromi Terawaki, Benoit M. Dawant, Robert L. Galloway and Michael I. Miga, "Incorporation of a laser range scanner into image-guided liver surgery: Surface acquisition, registration, and tracking," Med. Phys. 30 .7., July 2003.